2D.1 Numerical Study on the Development of Asymmetric Convection during Tropical Cyclone Landfall

Yubin Li * and Kevin K.W. Cheung

Department of Environment and Geography, Macquarie University, Sydney, New South Wales, Australia

1. INTRODUCTION

It has been observed and simulated in previous studies that landfalling tropical cyclones (TCs) develop asymmetry in convection, which is resulted from different momentum and heat fluxes between land and sea surface. However, there is no definite conclusion on the location of convection and how it is affected by land surface. Some previous studies indicated that convection was more concentrated in the front and on-shore flow quadrant (e.g. observations discussed in Yuan et al. 2009; simulations performed in Chen and Yau 2003), while others identified the maximum rainfall in the front and off-shore flow quadrant (e.g. observations in Li et al. 2012; simulations in Chan and Liang 2003). Dunn and Miller (1960) suggested that low-level convergence to the on-shore side of a TC track is more likely to be enhanced by the increased surface friction during landfall, and hence more rainfall. However, Wong and Chan (2007) pointed out that stronger surface convergence associated with the on-shore wind does not result in stronger planetary boundary layer (PBL) convergence at that location. In the present study, idealized numerical simulation using the Weather Research and Forecasting (WRF) model from the National Center for Atmospheric Research is performed to study the effects of land surface on the precipitation distribution of landfalling TCs.

2. MODEL SETUP

The simulation was on an f-plane at 15°S. There was quiescent environment only and without topography. Thirty-five vertical levels and three nested grids were used with the finest horizontal resolution of 4 km. The modified version of the Kain and Fritsch cumulus parameterization scheme was used for the two coarse domains but not the finest domain. Other physical packages included the WRF single-moment 6-class microphysics scheme with graupel and the MYNN PBL scheme. The methods of creating the base state of the atmosphere, the vortex and initial/boundary atmospheric conditions of the experiments followed those in Wong and Chan (2006). The land surface was placed 288 km south of the vortex center. The roughness length and moisture availability was fixed at 0.5 m and 5% over land, respectively.

*Corresponding author address: Yubin Li, Dept. of Environment and Geography, Macquarie University, Sydney, Australia. e-mail: yubin.li@mq.edu.au

3. SIMULATION RESULTS

3.1 Motion and Precipitation Patterns

The idealized axis-symmetric cyclone vortex was initially over the ocean, and then drifted to the land surface due to asymmetric flow developed within the vortex by the contrast between land and sea surface. The vortex center made landfall at 219.5 h with a motion speed of 1.4 m s^{-1} (Fig. 1).

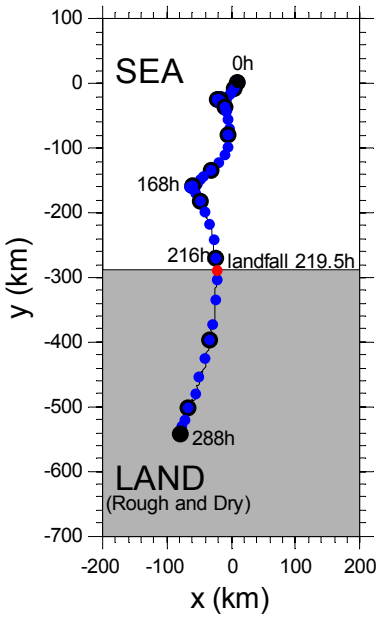

Fig. 1 Simulated track of the vortex, blue dots and black circles indicate 6-hourly and daily positions, respectively.

The reason for the on-shore drifting of the vortex was that the precipitation was stronger in the front quadrants (Fig. 3). The associated diabatic heating created a negative potential vorticity (PV) tendency there that moved the vortex toward land (Fig. 2).

However, horizontal advection also contributed similar magnitude as diabactic heating to the PV tendency, but vertical advection was comparatively smaller.

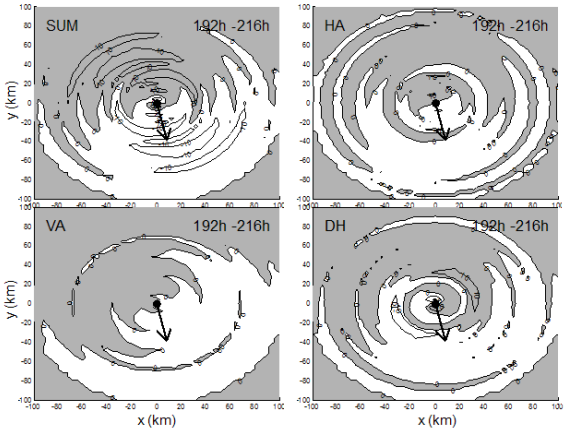

Fig. 2 Horizontal distribution of the terms in the Ertel's PV tendency equation at model level σ=0.5: Sum of all terms (top left; friction term neglected), horizontal advection (top right), vertical advection (bottom left), and diabatic heating (bottom right). Arrow in each panel is the vortex motion. Positive values are shaded (unit: 10^{-4} PVU s^{-1}).

The temporal variations of averaged precipitation in the inner-core (r<100km) and outer–band (100–300km) quadrants are shown in Fig. 3. It can be seen that during the first 120 h, the differences of precipitation in the four quadrants were small, but after 120 h there were more rainfall in the front quadrants. For most of the time, the front left (on-shore) quadrant experienced more rainfall than the front right (off-shore) quadrant. However, during 168 h–200 h that was before landfall, more rainfall occurred in the front right quadrant.

3.2 Convergence Patterns

The surface (10-m model layer) and PBL-top (model level σ=0.9) convergence two days before and after landfall (168 h–264 h) are examined (Fig. 4). It is found that for the surface inner core, convergence was stronger in the right quadrants before 216 h (just before landfall at 219.5 h), while afterward the differences in the four quadrants were not significant. Thus, before landfall the inner-core surface convergence was stronger in the off-shore flow side rather than the on-shore flow side. A possible explanation is that, before landfall surface winds were blocked by the enlarged roughness of land surface. Consequently, the inner-core surface winds ahead the motion turned inward and to the right, which made the winds stronger on the off-shore side. In other words, the land surface helped to convey the inner-core momentum from the front outer region to the off-shore flow region, which can be clearly seen from Fig. 5. At 210 h, the wind over land surface decreased in general but there was a wind maximum on the off-shore flow side of the vortex center.

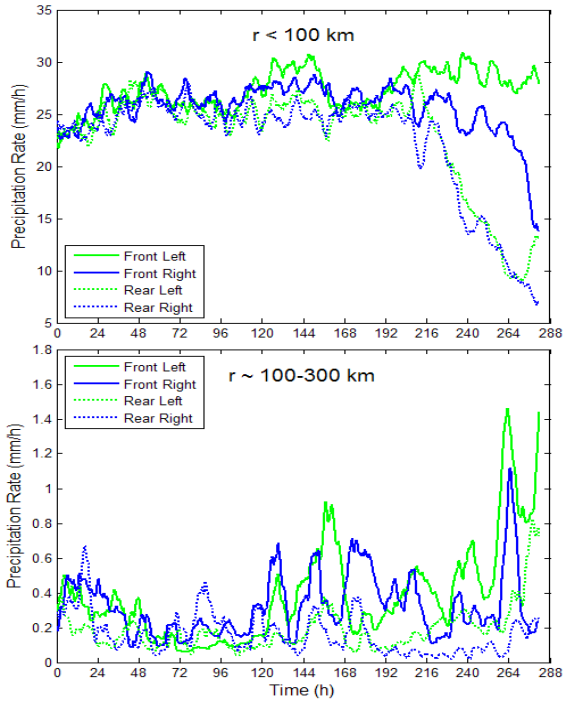

Fig. 3 Time series of the simulated averaged precipitation rate in the four quadrants with respect to motion direction.

The convergence in the surface outer-band region was strongly related to the on-shore flow position. It was stronger in the left quadrants before 240 h, and afterward shifted to the rear quadrants (Fig. 4). On the other hand, convergence at the inner-core PBL top was always stronger in the front quadrants, and shifted from front right to front left at 200 h. The convergence in the PBL-top outer-band region was most of the time stronger in right quadrants before 235 h, but afterward shifted to the front quadrants. The convergence pattern at the PBL top is consistent with the averaged precipitation pattern in Fig. 3, which

shows that for inner core more rainfall occurred in the front-right quadrant during 168 h to 200 h, and shifted to the front-left quadrant afterwards.

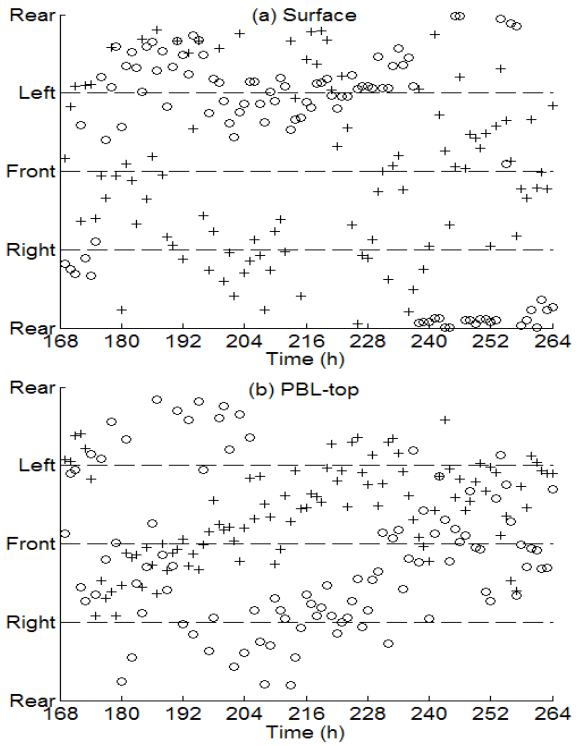

Fig. 4 Azimuthal location (relative to vortex motion) of the maximum wavenumber-1 component of the surface (top panel) and PBL-top (bottom panel) convergence in the inner-core (crosses) and outer-band region (circles).

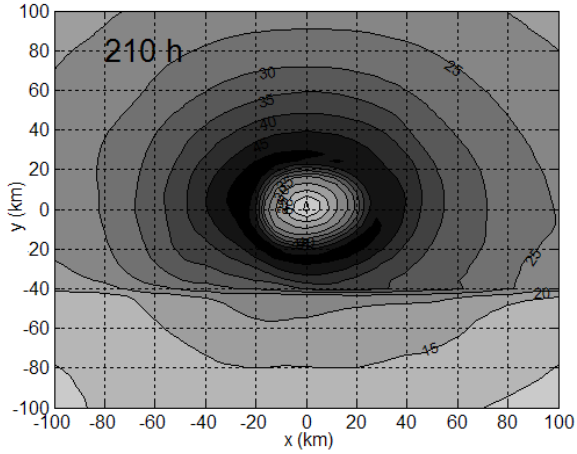

Fig. 5 Inner core surface wind speed (210 h).

To better illustrate the rainfall distribution associated with landfall, the accumulated precipitation during 168 h-264 h is shown in Fig. 6. Although the averaged precipitation in the front-right quadrant was less than that in the front left quadrant during landfall (216 h-222 h in Fig. 3), a rainfall maximum was located on the right side of the track in the inner-core region right at the coastline. This is consistent with the inner-core surface convergence pattern in Fig. 4 and the surface wind pattern in Fig. 5.

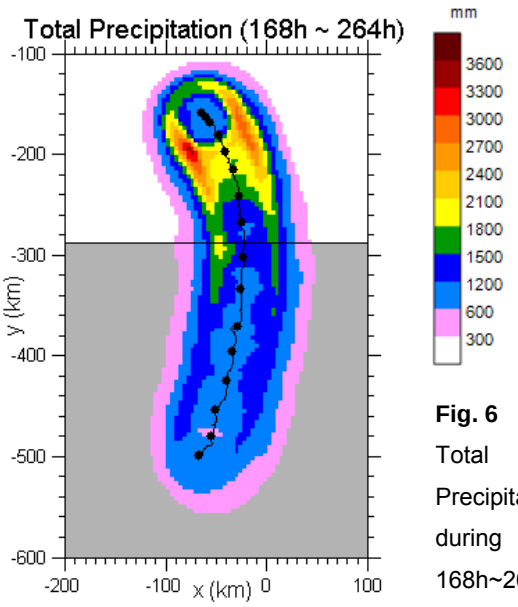

Fig. 6 Total Precipitation during 168h~264h.

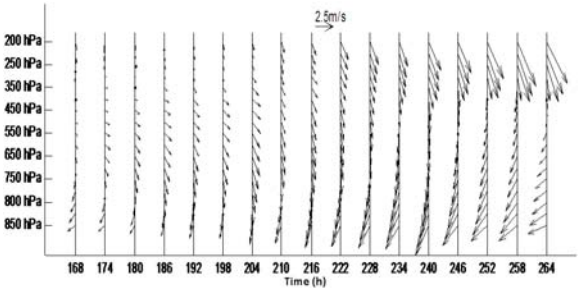

Fig. 7 Vertical and temporal variation of the averaged winds within 400 km from the vortex center.

3.3 Vertical Wind Shear (VWS)

The averaged winds within 400 km from vortex center from 850 hPa to 200 hPa is shown in Fig. 7, which shows that the low-level (750-850 hPa) winds had enhanced northeasterlies during landfall, while the upper-level (200-350 hPa) winds had enhanced northwesterlies. This pattern is similar with the observations in Li et al. (2012). Since quiescent environment was used in the model, it implies that the surface-induced asymmetry was not only confined to the low levels but has propagated to the upper levels through certain mechanisms. Note that a westerly VWS after landfall has been generated by the wind distribution.

With environmental VWS consideration, it has been demonstrated that more rainfall occurs in the down-shear quadrants (e.g., Corbosiero and Molinari 2003). In our simulation, more rainfall occurred in the up-shear side before 210 h for inner-core region and before 216 h for outer-band region (Fig. 8). Afterward rainfall was more concentrated in the down-shear right quadrant. That is, when asymmetry in the winds developed in the simulated TC vortex, the generated VWS acted like environmental shear and affected the subsequent rainfall distribution. Mechanisms such as this one are being verified by more simulations.

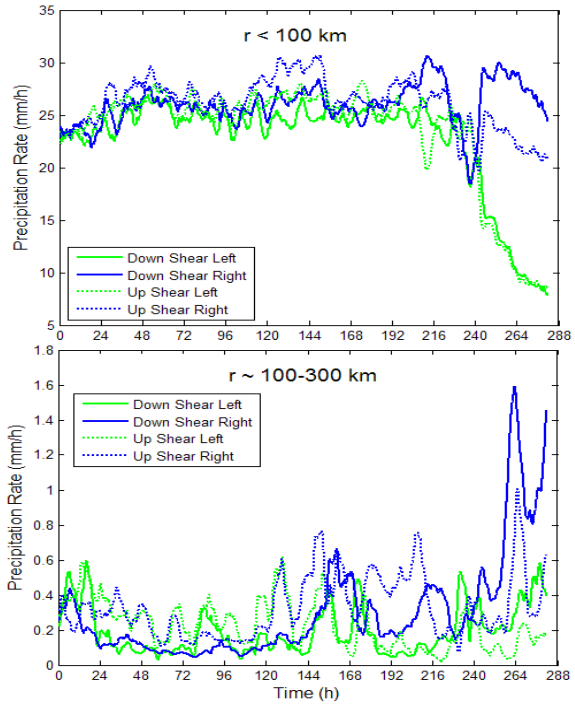

Fig. 8 Time series of the area averaged precipitation rate in the four quadrants with respect to the 200-850-hPa shear direction.

4. SUMMARY

A simulation of TC landfall under quiescent environment and the effects from land-sea surface contrast was performed with WRF model. It was found that horizontal advection (by land-induced asymmetric flow) and diabatic heating contributed to the motion of the vortex at similar magnitude. The precipitation in the inner core was stronger in the front-right quadrant one day before landfall, but afterward stronger rainfall shifted to the front-left quadrant. Although there was less moisture supply to the off-shore side, and hence weaker total rainfall in that area, the land surface helped to convey momentum from the front outer region to the off-shore side, and created stronger convergence and thus stronger rainfall maximum there. The surface-induced wind asymmetry was not confined to the lower levels but also propagated to the upper levels. Consequently, a westerly VWS after landfall was identified. More rainfall was found to be up–shear when the VWS was small before landfall, but changed to down-shear right when the VWS became larger after landfall.

References

Chan, J. C. L., and X. Liang, 2003: Convective asymmetries associated with tropical cyclone landfall. Part I: f-plane simulations. *J. Atmos. Sci.*, **60**, 1560–1576.

Chen, Y., M. K. Yau, 2003: Asymmetric Structures in a Simulated Landfalling Hurricane. *J. Atmos. Sci.*, **60**, 2294–2312.

Corbosiero, K. L., and J. Molinari, 2003: The relationship between storm motion, vertical wind shear, and convective asymmetries in tropical cyclones. *J. Atmos. Sci.*, **60**, 366–376.

Dunn, G. E., and B. I. Miller, 1960: Atlantic Hurricanes, Louisiana State University Press, 377 pp.

Li, Y., K.K.W. Cheung, J.C.L. Chan, and M. Tokuno, 2012: Rainfall distribution of five landfalling tropical cyclones in the northwestern Australian region. *Mon. Wea. Rev.* (submitted).

Wong, M. L. M., and J. C. L. Chan, 2006: Tropical cyclone motion in response to land surface friction. *J. Atmos. Phys.*, **63**, 1324–1337.

Wong, M. L. M., and J. C. L. Chan, 2007: Modeling the effects of land–sea roughness contrast on tropical cyclone winds. *J. Atmos. Sci.*, **64**, 3249–3264.

Yuan, J. N., W. Zhou, H. J. Huang, and F. Liao, 2009: Observational analysis of asymmetric distribution of convection associated with Tropical Cyclone Chuanchu and Prapiroon making landfall along the South China coast. *J. Trop. Meteor.*, **25**, 101–109.